The University of Osaka
Institutional Knowledge Archive

Title	High-resolution projection image reconstruction of thick objects by hard x-ray diffraction microscopy
Author(s)	Takahashi, Yukio; Nishino, Yoshinori; Tsutsumi, Ryosuke et al.
Citation	Physical Review B - Condensed Matter and Materials Physics. 2010, 82(21), p. 214102
Version Type	VoR
URL	https://hdl.handle.net/11094/86983
rights	Copyright 2010 by the American Physical Society
Note	

The University of Osaka Institutional Knowledge Archive : OUKA

https://ir.library.osaka-u.ac.jp/

The University of Osaka

High-resolution projection image reconstruction of thick objects by hard x-ray diffraction microscopy

Yukio Takahashi,[1,*] Yoshinori Nishino,[2] Ryosuke Tsutsumi,[3] Nobuyuki Zettsu,[4] Eiichiro Matsubara,[5] Kazuto Yamauchi,[3,4] and Tetsuya Ishikawa[6]

[1]*Frontier Research Base for Global Young Researchers, Frontier Research Center, Graduate School of Engineering, Osaka University, 2-1 Yamada-oka, Suita, Osaka 565-0871, Japan*
[2]*Research Institute for Electronic Science, Hokkaido University, Sapporo 001-0021, Japan*
[3]*Department of Precision Science and Technology, Graduate School of Engineering, Osaka University, 2-1 Yamada-oka, Suita, Osaka 565-0871, Japan*
[4]*Research Center for Ultra-precision Science and Technology, Graduate School of Engineering, Osaka University, 2-1 Yamada-oka, Suita, Osaka 565-0871, Japan*
[5]*Department of Materials Science and Engineering, Kyoto University, Yoshida, Sakyo, Kyoto 606-8501, Japan*
[6]*RIKEN SPring-8 Center, Kouto, Sayo-cho, Sayo-gun, Hyogo 679-5148, Japan*

Hard x-ray diffraction microscopy enables us to observe thick objects at high spatial resolution. The resolution of this method is limited, in principle, by only the x-ray wavelength and the largest scattering angle recorded. As the resolution approaches the wavelength, the thickness effect of objects plays a significant role in x-ray diffraction microscopy. In this paper, we report high-resolution hard x-ray diffraction microscopy for thick objects. We used highly focused coherent x rays with a wavelength of ∼0.1 nm as an incident beam and measured the diffraction patterns of a ∼150-nm-thick silver nanocube at the scattering angle of ∼3°. We observed a characteristic contrast of the coherent diffraction pattern due to only the thickness effect and collected the diffraction patterns at nine incident angles so as to obtain information on a cross section of Fourier space. We reconstructed a pure projection image by the iterative phasing method from the patched diffraction pattern. The edge resolution of the reconstructed image was ∼2 nm, which was the highest resolution so far achieved by x-ray microscopy. The present study provides us with a method for quantitatively observing thick samples at high resolution by hard x-ray diffraction microscopy.

PACS number(s): 07.85.−m, 42.30.−d, 61.46.−w

I. INTRODUCTION

X rays are a useful probe for characterizing bulk structures at high resolution because of their high penetration power and short wavelength. X-ray microscopy has particularly contributed to the visualization of interior structures buried within thick cells or bulk metals that are difficult to observe by the well-established method of electron microscopy. However, x-ray microscopy still lags behind electron microscopy in terms of resolution owing to the difficulty in fabricating x-ray lenses, although a 15 nm resolution has been achieved in a synchrotron experiment using a Fresnel zone plate.[1] To avoid this difficulty, a lensless x-ray microscopy combining coherent x-ray diffraction and the oversampling phasing method, i.e., x-ray diffraction microscopy, was proposed by Sayre[2] in 1980 and demonstrated by Miao *et al.*[3] in 1999. In this method, an object is illuminated with coherent x rays and its far-field diffraction pattern is recorded. An image of the object is reconstructed by applying iterative phasing methods[4–6] to the diffraction pattern. After the demonstration, important methods for the visualization of strain fields,[7] the observation of extended objects,[8,9] and the structural determination of single biomolecules[10] were developed. As a result, a number of application studies in materials science[11–15] and biology[16–20] have emerged.

The spatial resolution of x-ray diffraction microscopy is limited, in principle, by only the x-ray wavelength and the largest scattering angle recorded. The theoretically achievable resolution is half of the x-ray wavelength. However, it is difficult to achieve higher resolution since the diffraction intensity rapidly decays in accordance with a power law. The use of highly focused incident x-ray beams is effective for collecting higher angle diffraction data at a high signal-to-noise ratio. Recently, higher resolution x-ray diffraction microscopy has been realized using advanced x-ray focusing devices such as refractive lenses and total reflection mirrors. The spatial resolution has reached the sub-5-nm scale[21,22] in two dimensions and the sub-10-nm scale[15] in three dimensions.

Further improvement of the spatial resolution of x-ray diffraction microscopy remains a challenge. It is particularly discussed in application studies using x-ray free-electron lasers, such as the single-shot imaging of single biomolecules. Here, note that, as the resolution approaches the wavelength, the thickness effect of objects plays a significant role in x-ray diffraction microscopy.[23] In almost all coherent x-ray imaging studies, two-dimensional image reconstruction has been carried out on the basis of the projection approximation. The sample thickness is approximated to be zero, in other words, the propagation of the diffracted x rays inside the object is neglected. In a higher resolution scheme, one encounters the thickness effect and cannot use projection approximation. Thus, it is necessary to collect and handle diffraction data without neglecting the thickness effect.

In this paper, we report the highest-resolution projection image reconstruction of a thick metallic nanoparticle by hard x-ray diffraction microscopy, which is realized by both using high-density coherent x rays focused by total reflection mir-
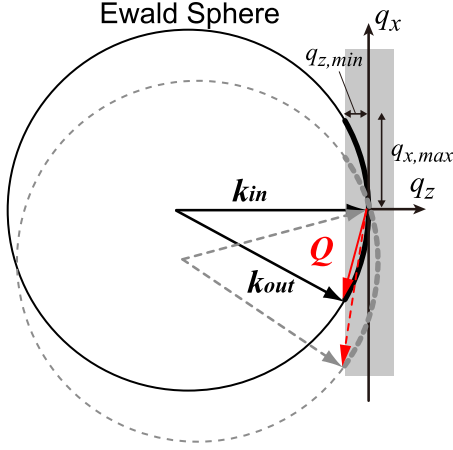
FIG. 1. (Color online) Schematic layout of the relationship between the Ewald sphere and Fourier space: the spatial distribution of speckles across the $q_z=0$ plane is schematically drawn using a gray square. The rotation of the scattering object in real space corresponds to the rotation of the Ewald sphere around the origin of the Fourier space. When the sample is tilted, higher q diffraction data in the $q_z \approx 0$ plane is observable, as shown by dotted lines.

rors and collecting diffraction data with the curvature of the Ewald sphere. The present study provides us with a method for quantitatively observing thick samples with high spatial resolution by x-ray diffraction microscopy.

II. THEORY

When an object with an electron density of $\rho(x,y,z)$ is illuminated by coherent x rays with plane waves and its far-field scattering waves satisfy the Born approximation, the magnitude of the structure factor $F(Q)$, where Q is the scattering vector, is equal to the magnitude of the Fourier transform of $\rho(x,y,z)$, which is expressed as

$$|F(Q)| = \left| \int \rho(x,y,z) e^{-i(q_x x + q_y y + q_z z)} dx dy dz \right|. \quad (1)$$

When diffraction, whose intensity is proportional to the square of $F(Q)$, is collected under an oversampling condition, $\rho(x,y,z)$ can be reconstructed by applying the phase retrieval algorithm to the diffraction pattern. When the reconstruction is carried out from the two-dimensional diffraction pattern in the $q_z=0$ plane, the reconstructed image corresponds to the projection of $\rho(x,y,z)$ through the z axis.

The observable coherent x-ray diffraction in the forward geometry can be understood from the arrangement of the Ewald sphere in Fourier space, as shown in Fig. 1. When diffracted photons are detected by a two-dimensional detector such as a charge-coupled device (CCD), the single diffraction pattern gives information on the Ewald surface in Fourier space. Chapman *et al.*[23] defined the numerical aperture of the diffraction microscope as

$$NA = q_{x,\max} \lambda, \quad (2)$$

where λ is the wavelength and $q_{x,\max}$ is the maximum lateral distance of the Ewald surface. As q_x increases, the observed
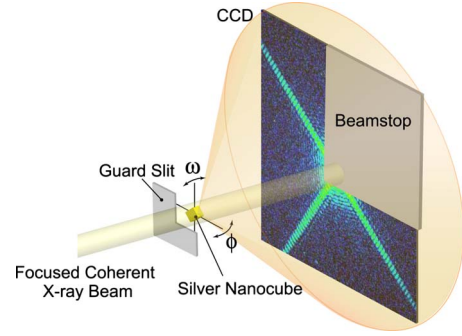

FIG. 2. (Color online) Schematic of the coherent x-ray diffraction experiment for collecting information on a cross section in Fourier space: focused coherent x rays with a wavelength of 0.1051 nm were radiated onto an isolated silver nanocube particle. To interrupt parasitic scattering x rays from the mirrors, guard slits were placed between the mirrors and the focus. Forward diffraction intensities were observed using a CCD detector. A direct x-ray beamstop was placed in front of the CCD detector. The incident x-ray angle was controlled by adjusting a two-axis rotational stage with angles of ϕ and ω.

information drifts away from the $q_z=0$ plane. The minimum longitudinal distance of the Ewald surface is expressed as $q_{z,\min} \approx -NA^2/2\lambda$. If the Ewald departure is half of the speckle half width, the permissible value of the sample thickness D is expressed as

$$D < \frac{\lambda}{2NA^2}. \quad (3)$$

For example, when one reconstructs images with a 1 nm resolution from a single diffraction pattern recorded using x rays with a wavelength of 0.1 nm, the samples that can be used are limited to objects thinner than 20 nm. Otherwise, by collecting a tilt series of diffraction pattern, the diffraction intensities have to be assemble through the origin of reciprocal space, which is equivalent to the standard precession method of x-ray crystallography.[24]

III. EXPERIMENTAL DETAILS

A silver nanocube with an edge length of ~150 nm was used as a sample, which was prepared by a modified version of the polyol synthesis technique developed by Xia and co-workers.[25] Sliver nanocubes are single crystals with a face-centered-cubic structure.[26] The nanocube was supported by a 100-nm-thick SiN membrane. Since the SiN membrane has an amorphous structure and a considerably uniform thickness, the small-angle intensities of x rays scattered from the membrane are much weaker than those of x rays scattered from the nanocube.

The experiments on coherent x-ray diffraction were performed at BL29XUL in SPring-8.[27] Figure 2 shows a schematic of the coherent x-ray diffraction experiment. The x-ray energy was tuned to 11.8 keV ($\lambda=0.1051$ nm) with an undulator gap and a Si (111) double-crystal monochromator. The x-ray beam was two dimensionally focused onto a spot of ~1 μm size by Kirkpatrick-Baez mirrors. An isolated
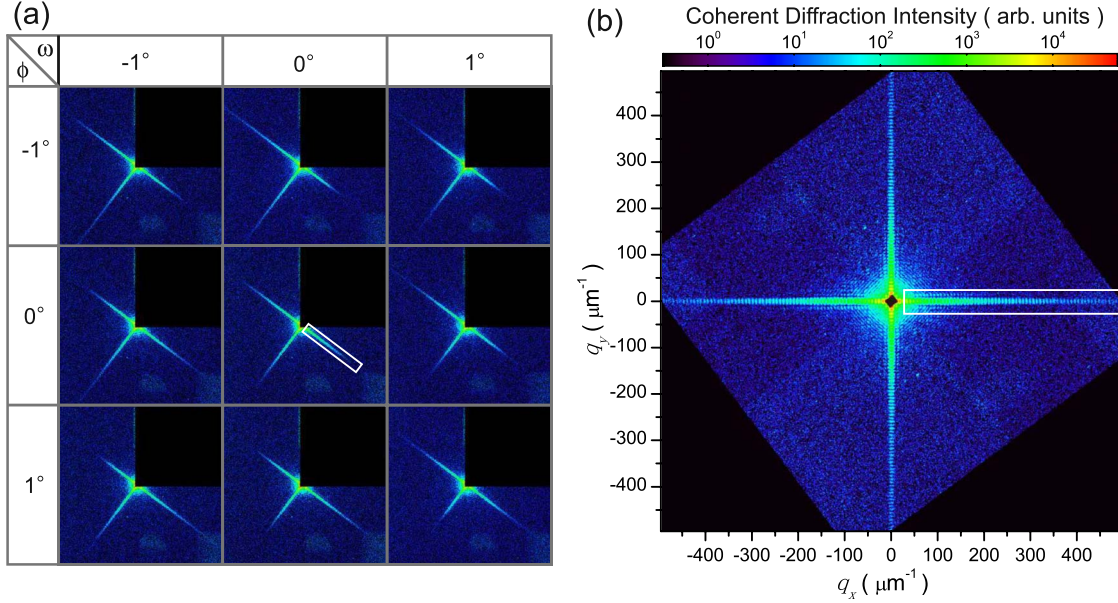
FIG. 3. (Color online) (a) Diffraction patterns of the silver nanocube at nine incident angles: each diffraction pattern is composed of an array of 1300×1340 pixels. (b) Diffraction pattern in the $q_z \approx 0$ plane derived from the nine diffraction patterns of (a). The total pixel number is 1611×1611. $\boldsymbol{q}$ is defined as $|\boldsymbol{q}| = 2 \sin(\Theta/2)/\lambda$, where Θ is the scattering angle and λ is the x-ray wavelength.

silver nanocube was placed at the focus and illuminated with the focused x-ray beam. The flux density at the focus was $\sim 1.0 \times 10^4$ photons/s/nm^2. Since the nanocube is much smaller than the focal spot, the illuminated x-ray beam is regarded as a plane wave. The diffracted x-ray photons were detected by an in-vacuum front-illuminated CCD detector with 1300×1340 pixels and pixel size of a 20×20 μm^2 placed 309 mm downstream. The position of the beamstop was adjusted so that the missing center of diffraction patterns becomes small.[22] The incident x-ray angle was controlled by adjusting a two-axis rotational stage, where ϕ and ω are the horizontal and vertical angles, respectively. At $(\phi, \omega) = (0°, 0°)$, the x-ray beam is entered into the vertical direction for the (001) plane of the nanocube. It is defined that $\boldsymbol{k}_{in}$ is parallel to $\boldsymbol{q}_z$ at $(\phi, \omega) = (0°, 0°)$.

According to the criterion given by Eq. (3), a single diffraction pattern provides a projection image with a resolution worse than ~ 2 nm under the present experimental conditions. When the incident x-ray angle is tilted by 1°, the Ewald sphere crosses speckles with a 1 nm resolution in the $q_z \approx 0$ plane. Data collection in the range from $-1°$ to $+1°$ for ϕ and ω provide information with a resolution better than 1 nm resolution in the $q_z \approx 0$ plane. In the present experiment, diffraction data were collected at nine incident angles: from $-1°$ to $+1°$ for ϕ and ω at 1° intervals. The x-ray exposure time at each angle was 180 s.

IV. RESULTS AND DISCUSSION

A. Diffraction pattern

Figure 3(a) shows the diffraction patterns of the silver nanocube at each angle. The black square in the upper right in each pattern is an unmeasured region due to the beamstop.

The diffraction patterns show a cross-shaped structure that result from the cubic shape of the particle. At $(\phi, \omega) = (0°, 0°)$, the contrast of speckle patterns in the upper left is almost equal to that in the lower right while that at the other angles is clearly different. For example, at $(\phi, \omega) = (-1°, 0°)$, speckle patterns in the upper left have a high contrast compared with those in the lower right. It has been reported that the centrosymmetry of speckle patterns decreases when the x-ray absorption and/or multiple scattering in an object is not negligible.[28–30] In the present experiment, the sample thickness is about 100 times less than the attenuation length at the present x-ray energy. In addition, the amount of x-ray absorption of the nanocube was $\sim 1\%$. The multiple scattering and the absorption effect are negligible. Thus, the asymmetric feature of the present diffraction patterns results from only the thickness effect (i.e., curvature of Ewald sphere).

Next, the diffraction pattern in the $q_z \approx 0$ plane was derived by patching the nine diffraction patterns in Fig. 3(a) on basis of the relationship between the Ewald sphere and the sample orientation. Part of the missing data due to the beamstop was interpolated using the centrosymmetry of the diffraction pattern. The area less than ~ 10 μm^{-1} remains as the missing center. Finally, the diffraction pattern was rotated so that the cross-shaped pattern became parallel to the q_x and q_y directions. Figure 3(b) shows the derived diffraction pattern in the $q_z \approx 0$ plane. On the other hand, the highest-q diffraction intensities were observed at 500 μm^{-1} ($\Theta = 3.01°$ and $NA = 0.053$), which means that structures were resolved with 1 nm resolution by x-ray diffraction analysis. In the present experiment, the observable highest-q diffraction was limited by the detector size.

Figures 4(a) and 4(b) show the enlarged images indicated by the white square in the pattern at $(\phi, \omega) = (0°, 0°)$ in Fig.

(a)

ω=0°, φ=0°

Patched pattern

q (μm^{-1})

(b)

Half period (nm)

Photon number (photon/pixel)

—— ω=0°, φ=0°

—— Patched pattern

q (μm^{-1})
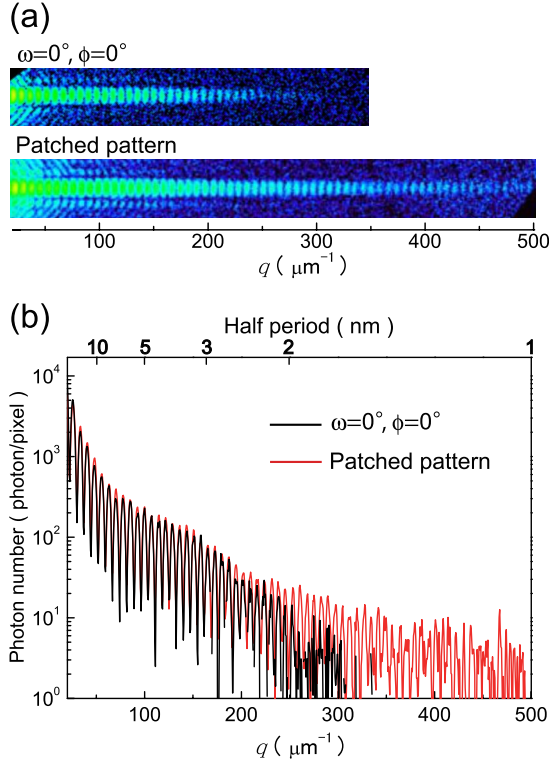
FIG. 4. (Color online) (a) Enlarged images of diffraction patterns at $(\phi, \omega) = (0°, 0°)$ of Fig. 3(a) and the patched pattern displayed in Fig. 3(b). Selected positions are indicated by white squares in Figs. 3(a) and 3(b), respectively. Cross-sectional plots through the peak top of the specles of (a).

3(a) and in the pattern in Fig. 3(b) and their cross-sectional plots through the peak top of speckles, respectively. The intensity of the patched diffraction pattern gradually decreases, similarly to the intensity distribution of Fraunhofer diffraction from a rectangular hole. On the other hand, the speckle intensities at $(\phi, \omega) = (0°, 0°)$ rapidly decay at more than 250 μm^{-1}. On the basis of Eq. (3), the sample thickness was estimated to be ~150 nm. This is the observation of a clear difference in coherent diffraction intensity due to only the thickness effect.

B. Reconstructed image

The projection image of a silver nanocube was reconstructed by the hybrid input-output method[5] with Shrinkwrap algorithm.[31] It is known that the phasing algorithm works well to estimate the missing central data. The iterative process started from a random electron-density map in a square support, and the support was revised iteratively every 1000 iterations using intermediately reconstructed images. Here, the support is a nonzero region in real space. In the iterative process, the electron density outside the support is forced to decrease gradually in real space and the measured coherent diffraction data is used in reciprocal space. The iterative process was continued for up to 2×10^3 iterations. Two-dimensional images of a silver nanocube were reconstructed starting from 100 different random electron-density maps,

(a)   (b)   (c)

P   2 nm
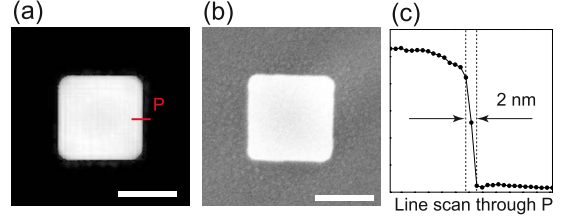
Line scan through P

FIG. 5. (Color online) (a) Projection image of the silver nanocube reconstructed from the diffraction pattern in Fig. 3(b). (b) SEM image of an identical silver nanocube. Scale bars in (a) and (b) correspond to 100 nm. (c) Cross-sectional plot through line P in (a).

and their images were averaged to obtain the final reconstruction.

Figures 5(a) and 5(b) show the final reconstructed image and a scanning electron microscopy (SEM) image of an identical nanocube before irradiating x rays, respectively. The reconstructed image corresponds to the projection of the electron density of the nanocube. The projection image is clearly visible and does not contradict the surface image obtained by SEM. The side of the square shape is ~150 nm, which is consistent with the thickness estimated from the intensity distribution of the diffraction pattern. Figure 5(c) shows a cross-sectional plot through line P indicated in Fig. 5(a). The edge resolution is 2.0 nm, which is slightly improved compared with our previous result.[22] However, it is worse than the resolution estimated from the diffraction pattern. The present high-q diffraction data suffer the signal loss due to the photon shot noise as shown in Fig. 4. It is thought that the degradation of the edge resolution is caused by the signal loss.[32]

V. CONCLUSION

We have presented a method of high-resolution hard x-ray diffraction microscopy for thick objects. To achieve higher resolution in x-ray diffraction microscopy, it is crucial not only to improve the flux density of coherent x rays but also to collect and handle the diffraction data which includes the thickness effect of objects. In this study, we used high-intensity x rays with a wavelength of ~0.1 nm produced by total reflection mirrors. Diffraction patterns of a silver nanocube with an edge length of ~150 nm were measured at various incident x-ray angles so as to fill a cross section in Fourier space. A diffraction pattern with information of 1 nm resolution was observed at a scattering angle of 3.01°. The diffraction pattern in the $q_z \approx 0$ plane was derived by patching nine diffraction patterns, and a projection image was then reconstructed through the z axis by the iterative phasing method. The edge resolution of the reconstructed image was ~2 nm, which was the highest resolution achieved by x-ray microscopy. We believe that the present results will pave the way for the quantitative observation of thick objects with a high spatial resolution and the subsequent investigation of a wide range of materials and biological systems.

*Corresponding author; takahashi@wakate.frc.eng.osaka-u.ac.jp

[1] W. Chao, B. D. Harteneck, J. A. Liddle, E. H. Anderson, and D. T. Attwood, Nature (London) **435**, 1210 (2005).

[2] D. Sayre, in *Imaging Processes and Coherence in Physics*, Springer Lecture Notes in Physics Vol. 112, edited by J. Schlenker, M. Fink, J. P. Goedgebuer, V. Malgrange, J. C. Viénot, and R. H. Wade (Springer, Berlin, 1980), pp. 229–235.

[3] J. Miao, P. Charalambous, J. Kirz, and D. Sayre, Nature (London) **400**, 342 (1999).

[4] R. W. Gerchberg and W. O. Saxton, Optik (Stuttgart) **35**, 237 (1972).

[5] J. R. Fienup, Appl. Opt. **21**, 2758 (1982).

[6] V. Elser, J. Opt. Soc. Am. A **20**, 40 (2003).

[7] M. A. Pfeifer, G. J. Williams, I. A. Vartanyants, R. Harder, and I. K. Robinson, Nature (London) **442**, 63 (2006).

[8] J. M. Rodenburg, A. C. Hurst, A. G. Cullis, B. R. Dobson, F. Pfeiffer, O. Bunk, C. David, K. Jefimovs, and I. Johnson, Phys. Rev. Lett. **98**, 034801 (2007).

[9] H. M. Quiney, A. G. Peele, Z. Cai, D. Paterson, and K. A. Nugent, Nat. Phys. **2**, 101 (2006).

[10] H. N. Chapman, A. Barty, M. J. Bogan, S. Boutet, M. Frank, S. P. Hau-Riege, S. Marchesini, B. W. Woods, S. Bajt, W. H. Benner, R. A. London, E. Plönjes, M. Kuhlmann, R. Treusch, S. Düsterer, T. Tschentscher, J. R. Schneider, E. Spiller, T. Möller, C. Bostedt, M. Hoener, D. A. Shapiro, K. O. Hodgson, D. V. D. Spoel, F. Burmeister, M. Bergh, C. Chaleman, G. Huldt, M. M. Seibert, F. R. N. C. Maia, R. W. Lee, A. Szöke, N. Timneanu, and J. Hajdu, Nat. Phys. **2**, 839 (2006).

[11] J. Miao, C.-C. Chen, C. Song, Y. Nishino, Y. Kohmura, T. Ishikawa, D. Ramunno-Johnson, T.-K. Lee, and S. H. Risbud, Phys. Rev. Lett. **97**, 215503 (2006).

[12] Y. Takahashi, Y. Nishino, T. Ishikawa, and E. Matsubara, Appl. Phys. Lett. **90**, 184105 (2007).

[13] B. Abbey, G. J. Williams, M. A. Pfeifer, J. N. Clark, C. T. Putkunz, A. Torrance, I. McNulty, T. M. Levin, A. G. Peele, and K. A. Nugent, Appl. Phys. Lett. **93**, 214101 (2008).

[14] M. C. Newton, S. J. Leake, R. Harder, and I. K. Robinson, Nature Mater. **9**, 120 (2010).

[15] Y. Takahashi, N. Zettsu, Y. Nishino, R. Tsutsumi, E. Matsubara, T. Ishikawa, and K. Yamauchi, Nano Lett. **10**, 1922 (2010).

[16] J. Miao, K. O. Hodgson, T. Ishikawa, C. A. Larabell, M. A. LeGros, and Y. Nishino, Proc. Natl. Acad. Sci. U.S.A. **100**, 110 (2003).

[17] D. Shapiro, P. Thibault, T. Beetz, V. Elser, M. Howells, C. Jacobsen, J. Kirz, E. Lima, H. Miao, A. M. Neiman, and D. Sayre, Proc. Natl. Acad. Sci. U.S.A. **102**, 15343 (2005).

[18] C. Song, H. Jiang, A. Mancuso, B. Amirbekian, L. Peng, R. Sun, S. S. Shah, Z. H. Zhou, T. Ishikawa, and J. Miao, Phys. Rev. Lett. **101**, 158101 (2008).

[19] Y. Nishino, Y. Takahashi, N. Imamoto, T. Ishikawa, and K. Maeshima, Phys. Rev. Lett. **102**, 018101 (2009).

[20] K. Giewekemeyer, P. Thibault, S. Kalbfleisch, A. Beerlink, C. M. Kewish, M. Dierolf, F. Pfeiffer, and T. Salditt, Proc. Natl. Acad. Sci. U.S.A. **107**, 529 (2010).

[21] C. G. Schroer, P. Boye, J. M. Feldkamp, J. Patommel, A. Schropp, A. Schwab, S. Stephan, M. Burghammer, S. Schoder, and C. Riekel, Phys. Rev. Lett. **101**, 090801 (2008).

[22] Y. Takahashi, Y. Nishino, R. Tsutsumi, H. Kubo, H. Furukawa, H. Mimura, S. Matsuyama, N. Zettsu, E. Matsubara, T. Ishikawa, and K. Yamauchi, Phys. Rev. B **80**, 054103 (2009).

[23] H. N. Chapman, A. Barty, S. Marchesini, A. Noy, S. P. Hau-Riege, C. Cui, M. R. Howells, R. Rosen, H. He, J. C. H. Spence, U. Weierstall, T. Beetz, C. Jacobsen, and D. Shapiro, J. Opt. Soc. Am. A **23**, 1179 (2006).

[24] B. E. Warren, *X-ray Diffraction* (Dover, New York, 1969).

[25] S. H. Im, Y. T. Lee, B. Wiley, and Y. Xia, Angew. Chem., Int. Ed. **44**, 2154 (2005).

[26] Y. Sun and Y. Xia, Science **298**, 2176 (2002).

[27] K. Tamasaku, Y. Tanaka, M. Yabashi, H. Yamazaki, N. Kawamura, M. Suzuki, and T. Ishikawa, Nucl. Instrum. Methods Phys. Res. A **467-468**, 686 (2001).

[28] C. C. Retsch and I. McNulty, Phys. Rev. Lett. **87**, 077401 (2001).

[29] C. Song, R. Bergstrom, D. Ramunno-Johnson, H. Jiang, D. Paterson, M. D. deJonge, I. McNulty, J. Lee, K. L. Wang, and J. Miao, Phys. Rev. Lett. **100**, 025504 (2008).

[30] Y. Takahashi, H. Kubo, H. Furukawa, K. Yamauchi, E. Matsubara, T. Ishikawa, and Y. Nishino, Phys. Rev. B **78**, 092105 (2008).

[31] S. Marchesini, H. He, H. N. Chapman, S. P. Hau-Riege, A. Noy, M. R. Howells, U. Weierstall, and J. C. H. Spence, Phys. Rev. B **68**, 140101(R) (2003).

[32] X. Huang, H. Miao, J. Steinbrener, J. Nelson, D. Shapiro, A. Stewart, J. Turner, and C. Jacobsen, Opt. Express **17**, 13541 (2009).